

Intra-seasonal variability of cloud amount over the Indian subcontinent during the monsoon season as observed by TRMM precipitation radar

*Subhendu Brata Saha*¹, *Soma Sen Roy*¹, *S. K. Roy Bhowmik*¹
and *P. K. Kundu*²

¹India Meteorological Department, India

²Jadavpur University, Department of Mathematics, West Bengal, India

Received 26 November 2013, in final form 23 May 2014

The intra-seasonal variability of the Indian summer monsoon, which manifests in the form of “active” and “break” phases in rainfall, is investigated with respect to the variability of the convective and stratiform precipitating cloud pattern over the region. Long period data from TRMM PR satellite (2A23 and 3B42 datasets) for the monsoon season of 2002 to 2010 over the Indian subcontinent is used for this purpose. The study reveals that the most significant spatial variation in convective and stratiform cloud amount in relation to the active and break phase occurs over the monsoon trough region in central India. The active phase is characterized by positive convective (~5%) and stratiform (~20%) precipitating cloud anomalies over this region. However, the maximum of the former precedes the latter by 1–2 days leading up to the active phase, indicating that the stratiform build up, is due to the gradual organization of the convective cloud systems over the region. The days leading up to the break phase are marked by negative anomalies in the convective and stratiform fractions of cloudiness over this region, which are in phase with each other, unlike the lead-up to the active phase. Analysis of the pattern of atmospheric heat source and sinks over the region from the NCEP–NCAR re-analysis data indicates that the engine for the growth/decay of convection over the monsoon trough region lies primarily in the Bay of Bengal and adjacent east India. The active phase is preceded by a heating pattern that promotes large scale, organized convective cloud growth over the Bay of Bengal preceding the actual onset, while the heating pattern leading up to the break phase promotes the formation of isolated convective clouds and decay of cloud organization over the monsoon trough region.

Keywords: intra-seasonal variability, TRMM Precipitation Radar; Indian summer monsoon, active break phases, convective cloud, stratiform cloud, heat source, heat sink.

1. Introduction

Indian summer monsoon (ISM) is characterized by seasonal changes in atmospheric circulation and precipitation associated with the asymmetric heating of land and sea. This season accounts for 75 per cent of the annual rainfall for most of India (Raghavan, 1967). While large-scale synoptic features of the monsoon season over India repeat from year to year, these features have significant intraseasonal variability and the associated rainfall varies in space and time, leading to floods and droughts over large areas (Ananthkrishnan, 1977). It is significant that, the spatial pattern of intra-seasonal variability of ISM rainfall does not show any remarkable interannual variability (Krishnamurthy and Shukla, 2000). The quasi-periodic intraseasonal variability of the ISM, which is in the form of systematic and significantly enhanced and reduced rainfall activity over the Indian region gives rise to “active” and “break” phases of ISM rainfall (Krishnamurthy and Bhalme, 1976; Gadgil, 2003).

The active (break) spell of ISM is associated with the intensification (suppression) of deep convective systems over the monsoon trough region (Sikka and Gadgil, 1980; Yasunari, 1980). The active phase is characterized by above normal rainfall over central India and below normal over northern India (foothills of the Himalaya) and southern India and vice-versa during the break phase (Krishnamurthy and Shukla, 2000; Krishnan et al., 2000). An extensive study of Ramamurthy (1969) using Indian rainfall data reveals that during “break” phase, the Continental Tropical Convergence Zone (CTCZ) is shifted northward from its normal position to the foothills of the Himalayas, and the rainfall activity increases over south-eastern peninsular India during the same period. While the general pattern of convection associated with the onset of active and break phases of ISM is systematic, it should also be noted that the reason for the occurrence of individual active and break spells and the transitions between the spells are far more complex to understand (Webster et al., 1998). Hence the study aims at understanding the average behaviour of the intra-seasonal variability of ISM.

The heating profile of the atmosphere during the monsoon season has long been used to understand the intraseasonal variability of rainfall during the ISM. Annamalai et al. (1999) concluded that, in terms of seasonal mean climatologies of precipitation, the European Centre for Medium-Range Weather Forecasts (ECMWF) Reanalysis (ERA) is better than other models due to its ability to simulate the south Asian monsoon rainfall. This is because of its ability to simulate better the day-to-day variation of the diabatic heating field over the monsoon domain. Hence the intra-seasonal variability of the heating profile of the atmosphere has to be studied in detail with a sufficiently long observation dataset, to correctly model it into General Circulation Models (GCM) models.

A good estimate of the heating profile of the atmosphere can be obtained from the cloud cover over the region. METEOSAT satellite data reveal that while the active phase is associated with dense deep convection over the monsoon trough region, an abrupt atmospheric drying in the middle and upper troposphere (be-

tween 600 and 200 hPa) occurs three days prior to the commencement of break, which limits the growth of deep cumulus clouds over this region, thereby leading to a transition from active to break monsoon phase (Rao et al., 2004). Using MODIS data of 8 years (2000–2007), an inverse relationship was found to exist between the cloud properties of the monsoon zone over central India and the southeast equatorial Indian Ocean, suggesting a possible role of the southeast equatorial Indian Ocean in the development of active-break cycles (Ravi Kiran et al., 2009). Later studies of the heating profile of the atmosphere in relation to convection have been based on the data of microwave sensors on-board TRMM and CLOUDSAT satellites. These studies have separated the clouds into two types – convective and stratiform. The net heating profile of the atmosphere in the stratiform component of cloud systems is distinctly different from that in the convective cloud region (Houze, 1982; 1989). The heating associated with convective rain is positive throughout the profile, whereas, the heating is concentrated in the upper troposphere for stratiform rain, which implies a stronger upper-level heating response (Houze et al. 1980; Johnson et al., 1999). The relative fractions of convective and stratiform cloudiness in the total cloud amount over a region, is an indicator of the level where heating is maximum over the region. Previous studies have reported of the importance of stratiform heating on the evolution of tropical low-frequency intraseasonal oscillations (e.g., Chattopadhyay et al., 2009). With the availability of long period dataset of the TRMM satellite, with algorithms to reliably identify convective and stratiform cloudiness, it is now possible to construct composites of the relative stratiform and convective fractions of cloudiness over the Indian region delineating the intraseasonal variability of the atmosphere over the Indian region.

The purpose of the present study is to examine the observed anomalous heating profiles of the atmosphere in the CTCZ region during and leading up to the active and break phases of the ISM. This is sought to be inferred from the long period cloud observational 2A23 dataset (2002–2009) of the Precipitation Radar on board the TRMM satellite. The results are independently validated with the data from the NCEP re-analysis dataset for the same period. Both the observation and model re-analysis datasets are then used to understand the changes in the diabatic profile of the atmosphere before, during, and following the active and break phases of the ISM.

The paper is organized as follows. The data used in this study and the methods of data processing are briefly described in section 2. Results and discussions are in section 3 and conclusions are summarized in section 4.

2. Datasets and methodology

2.1. Identifying active and break phases

The study period encompasses the monsoon periods (1 June to 30 September) of 9 years, from 2002 to 2010. This includes 3 deficient ISM rainfall (10% less than the Long-Period average, LPA) years (2002, 2004 and 2009) and normal

ISM rainfall for the other 6 years with respect of total seasonal monsoon rainfall over the India as a whole (source: IMD South-West monsoon review documents from 2002 to 2010). Traditionally, operational forecasters of the India Meteorological Department (IMD) identify active and break events, based on low level pressure field and wind pattern over the Indian region. These phases are often defined, only after the monsoon flow has established over the entire Indian region to account for fluctuations in the intensity of rainfall in the seasonal transitions, i.e., onset and retreat phases of the monsoon (Rajeevan et al., 2010). Previous studies for identifying active and break phases of ISM, have been based on quantitative measurement of the rainfall over the monsoon trough region. An excess (deficient) rainfall phase over this region signifies active (break) phase of ISM rainfall (Rao et al., 2004). Gadgil and Joseph (2003) also considered the similar homogeneous area of rainfall anomaly for identifying active and break periods. Recently Rajeevan et al. (2010) suggested a new quantitative criterion for identifying active and break events from the high resolution daily gridded average rainfall data over a critical area, called the Core Monsoon Region (CMR), which corresponds to the area bounded by 65–88° E and 18–25° N (Fig. 1), within which the CTCZ normally fluctuates in the peak monsoon months of July and August. As per their methodology, the active (break) events are identified as periods during which, the normalized positive (negative) anomaly of the rainfall over the core monsoon region exceeds +1 (–1) standard deviation about the mean, and provided the criterion is satisfied for at least three consecutive days. Their study showed that the inter-annual variation of the all-India summer monsoon rainfall (ISMR) is highly correlated (correlation coefficient: 0.91) with that of the summer monsoon rainfall over the core monsoon zone suggesting that it is a critical region for the interannual variation. The quantitative nature of this criterion for categorizing intraseasonal variability of the ISM, as well as its consonance with

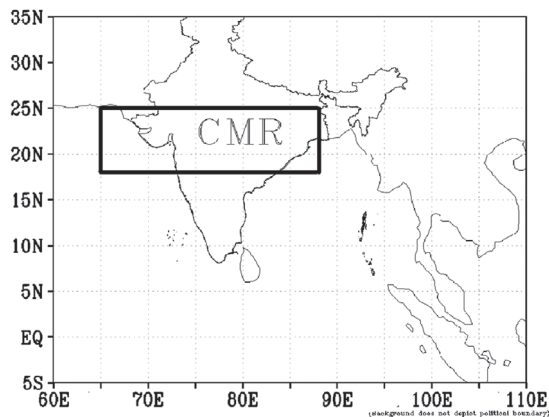


Figure 1. Domain of analysis for this study. The Core Monsoon Region (65–88° E, 18–25° N) is delineated by a black box.

forecasters' observations and previous results of active and break phases based on synoptic analysis of weather patterns, makes it the method of choice for identifying the phases of the ISM while analyzing the intraseasonal variability of the ISM (e.g., Manoj et al., 2011). We have hence, used their definition of the periods of active and break phases of the monsoon rainfall for the nine years. During the July and August of this 9 years period of study there were in total 74 active and 93 break days. The active periods were most frequent during 2006 (four events), while they were absent during 2002. On the other hand, out of total fourteen break events, a maximum of three events was observed in 2004 and no break event was observed in 2003 and 2006. The specific active and break events during the nine years considered in this study is displayed in Table 1 (from Rajeevan et al., 2010 and 2013).

2.2. TRMM dataset and its processing

Two products of the Tropical Rainfall Measuring Mission (TRMM) have been used in this study (Kummerow et al., 1998). The rainfall amount over the core monsoon region is measured using the TRMM 3B42 V6 (or TMPA) rainfall da-

Table 1. Active and break periods during 2002 to 2010 [Source: (a) 2002 to 2007 – Rajeevan et. al., 2010; (b) 2008 to 2010 – Rajeevan et. al., 2013].

Year	Active Spell		Break Spell	
	Date	No. of Days	Date	No. of Days
2002	-	0	04–17 JUL 21–31 JUL	25
2003	26–28 JUL	3	-	0
2004	30 JUL–01AUG	3	10–13JUL 19–21JUL 26–31 AUG	13
2005	01–04 JUL 27 JUL–01 AUG	10	07–14 AUG 24–31 AUG	16
2006	03–06 JUL 28 JUL–02 AUG 05–07 AUG 13–22 AUG	23	-	0
2007	01–04 JUL 06–09 JUL 06–09 AUG	12	18–22 JUL 15–17 AUG	8
2008	27–29 JUL 09–12 AUG	7	14–19 JUL 21–24 AUG	10
2009	12–16 JUL 19–23 JUL	10	29 JUL–10 AUG 16–19 AUG	17
2010	01–03 AUG 05–07 AUG	6	17–20 JUL	4
Total	Active days:	74	Break days:	93

taset for the monsoon period of 2002 to 2010 (Huffman et al., 2007). While rainfall was also available from the corresponding 2A25 dataset of the TRMM satellite, the 3B42 dataset provides uniform grid point data every three hours from geostationary satellites. This avoids the sampling error problems inherent to the data from polar orbiting satellites. The validation of this rainfall product for the ISM, using the 1° gridded raingauge rainfall product of IMD, demonstrates that TMPA reasonably depicts the pattern and intensity of individual monsoon low-pressure systems and depressions (Rahman et al., 2009). Other studies show that the TMPA estimates over the Western Ghats are most accurate over regions of moderate rainfall and mainly inaccurate in regions of sharp rainfall gradient (Nair et al., 2009). In view of the above findings, the TMPA product is a reasonable estimate of the rainfall over the Indian region. The three hourly rainfall values are accumulated in 0.25° grid boxes for the entire Indian region throughout the day to obtain daily values. This is then used to calculate the average daily rain rate (per hour) at each 0.25° grid box. This dataset is used for computing composite rainrate for each phase of the ISM, over the Indian region.

The other TRMM product used in this study, is the 2A23 (version 7) dataset, for the monsoon period of 2002 to 2010. The TRMM 2A23 product, which is at 5 km × 5 km resolution, is created by merging convective–stratiform separation methods, based on the vertical structure of the echoes from the Precipitation Radar (brightband identification, echo-top height, and maximum reflectivity in the vertical profile; Awaka et al., 1997) and on horizontal variability of the echo (peakedness and local echo intensity; Steiner et al., 1995). This algorithm classifies the PR echoes at each 5km pixel into three categories: “convective”, “stratiform”, and “other” based on the horizontal and vertical echo structure. The “other” category represents either noise or regions of precipitation aloft with no precipitation near the surface. The ambiguity of the “other” category and its very small contribution to total rainfall, implies that we can neglect “others” as was done by Schumacher and Houze (2003). Further details of the PR 2A23 algorithm are available online at <http://daac.gsfc.nasa.gov/>.

The TRMM 2A23 product data was first remapped into a regular latitude-longitude grid at 0.25° lat–lon resolution over the Indian region using a nearest-neighbor approach (Romatschke et al., 2010). The 2A23 data pixels for each cloud type are accumulated over the Indian subcontinent for all the orbital overpasses (domain latitude from 25.0° S to 35.0° N and longitude from 30.0° E to 120.0° E) separately, for the active and break phases for the period of study. Remapping such a high resolution orbital data and creating composites may introduce some unavoidable sampling errors (Nesbitt and Anders, 2009). However, this is also true with the generation of other high resolution Level 3 climate products from TRMM data, such as 3A25 dataset. As Nesbitt and Anders (2009) pointed out, the observed sampling error is a function of resolution, rain rate and sampling frequency. The sampling errors may be avoided by increasing the box size, or accumulating for longer intervals. As already mentioned in the earlier section, the active or break phase of the monsoon is defined by constant weather condi-

tions over the Indian subcontinent throughout the period. Hence, we may presume that the cloud pattern to remain constant during these periods. This allows us to sum over the pixels corresponding to orbital overpasses during the entire active/break period to obtain larger number of samples per grid box. The missing values (without any scan) are treated separately and they are set to -99.9 . By this method of compositing, we ensure that each grid box is sampled more than 1000 in the active/ break composites. To address the geographical inhomogeneity of sampling, these composite data counts for each cloud type are normalized by dividing convective and stratiform pixel count of a grid box by the total scan pixel count of that grid box and multiplying by 100 to get the percentage value of convective / stratiform fraction of that grid box. Since these phases are spread over nine years, the diurnal bias in the sampling is also another likely source of error (Negri et al., 2002 and Bowman et al., 2005). We expect the benefits of having such a high-resolution dataset to outweigh the disadvantage of some statistical fluctuations since the horizontal gradients and temporal scale of precipitation over this region during the monsoon season, are probably much larger than the sampling errors (Anders et al., 2006; Romatschke and Houze, 2011). Also Schumacher and Houze (2003) and Bell and Kundu (2000) have suggested that 0.6 m/year rain accumulation threshold gives less noisy results. Most of the Indian region except the western most part of India receives more than 0.6 m/year (Pokhrel and Sikka, 2013). Thus, the uncertainty from this sampling is minimum in our study region.

2.3. Computing heat source ($Q1$) and moisture sink ($Q2$)

To validate the information of the heating profile as obtained from the cloud type ratio over the region, the apparent heat source ($Q1$) and moisture sink ($Q2$) profiles (Yanai et al., 1973) have been computed for the monsoon period of 2002–2010 from the National Centers for Environmental Prediction–National Center for Atmospheric Research (NCEP–NCAR) daily mean reanalysis data (Kalnay et al., 1996). The daily data are at $2.5^\circ \times 2.5^\circ$ grid resolution and includes zonal wind component (U), meridional wind component (V), vertical wind (ω), temperature (T) and specific humidity (q) for 12 pressure levels (1000, 925, 850, 700, 600, 500, 400, 300, 250, 200, 150, 100 hPa). Following Luo and Yanai (1984), Bhide et al. (1997) and the TOGA-COARE (Tropical Ocean Global Atmosphere – Coupled Ocean Atmosphere Response Experiment) website <http://kiwi.atmos.colostate.edu/scm/toga-coare.html> the $Q1$ and $Q2$ values are computed from:

$$\frac{Q1}{C_p} = \frac{dT}{dt} + h(T) + \left(\frac{P}{P_0}\right)^k \cdot \omega \cdot \frac{d\theta}{dP} \quad (1)$$

$$\frac{Q2}{C_p} = -\frac{L_v}{C_p} \left[\frac{dq}{dt} + h(q) + v(q) \right] \quad (2)$$

where C_p is the specific heat of dry air at constant pressure, T is the temperature, t is the time, $h(T)$ is the horizontal advection of T , P the pressure, P_0 is the 1000 hPa pressure level, ω is the vertical velocity in p -coordinates, $k (=R_d/C_p)$ is the ratio of the gas constant of dry air (R_d) and specific heat of dry air at constant pressure (C_p), θ is the potential temperature, L_v is the latent heat of vaporization at 0 °C, q is the specific humidity, $h(q)$ the horizontal advection of q , $v(q)$ the vertical advection of q . The daily $Q1$ and $Q2$ values in K/day are computed at the resolution of the re-analysis dataset for the whole domain and span of the study. The values of $Q1$ and $Q2$ have been computed considering 1000 hPa level as base level. The mean value of the $Q1$ and $Q2$ parameters have been computed at each grid point, for the entire period (monsoon seasons from 2002–2010) for all standard levels. Anomalies of the composite active and break phases have been computed for all levels over the CMR region to match the corresponding cloud anomalies.

2.4. Creating lead lag composite

To understand the onset and withdrawal of the active/break phases, a pseudo time sequence of TRMM 3B42 and 2A23 datasets (at 0.25° resolution) and $Q1$ and $Q2$ (at 2.5° resolution) has been constructed for the Indian region, preceding and following the active and break phases of all the monsoon seasons during the period 2002 to 2010. As already stated, since forecasters identify the active/break phase of ISM by common features for the region during the entire period, the data for the entire active / break spell is accumulated together as the reference time (as day 0). Preceding and following the active (break) phase in rainfall, the cloud fraction data derived from 2A23 dataset are accumulated as a three day running mean. The first lead (lag) day is created by compositing three days prior to (following) the occurrence of the active/break phase including the commencement (cessation) day. The second lead day is created by creating an average of three days consisting of active (–3) to active (–1) days, while the second lag day is created from the average for three consecutive days consisting of active (+1) to active (+3) days. In this way, up to five lead and lag day products are created for the active/break phases. However, these lead/lag days are selected such that none of the day overlap with following or preceding active or break events. This procedure for three day lead-lag composites smoothens the variation of the cloud fractions leading to and following the active/break episodes. It also increases the scan count per grid box (a minimum of 200 samples) to obtain more stable outputs. The rain rate (3B42) lead-lag composites are computed as daily values, such as the first lead (lag) is created by compositing daily data for one day prior to (following) the occurrence of the active/break phase. Day 2 is created compositing daily data for two days prior to (following) the active/break phase and so on. These values are plotted and displayed in Fig. 4.

The heat source ($Q1$) and moisture sink ($Q2$), calculated using NWP model output (NCEP-NCAR reanalysis data), are also composited and averaged over

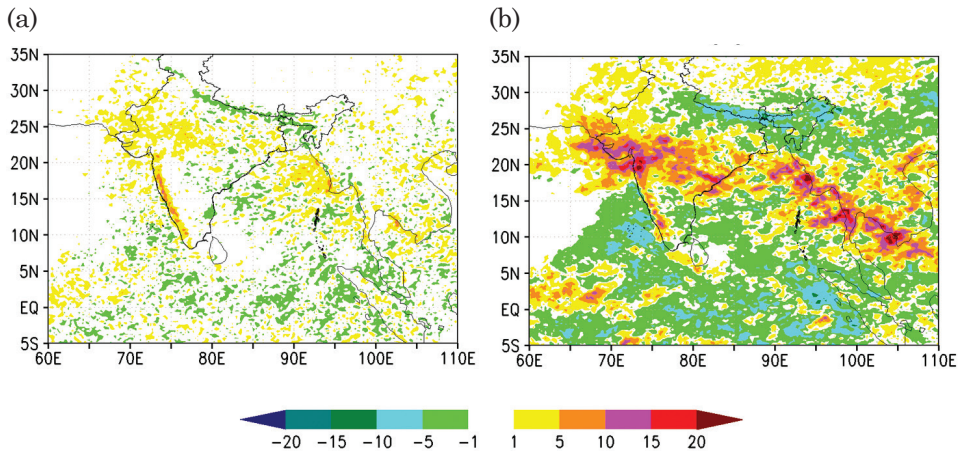


Figure 2. (a) Convective and (b) stratiform anomaly derived from 2A23 data, composited for active monsoon phases during July and August for the period 2002–2010. The anomalies of echo fractions are shown as percentage value.

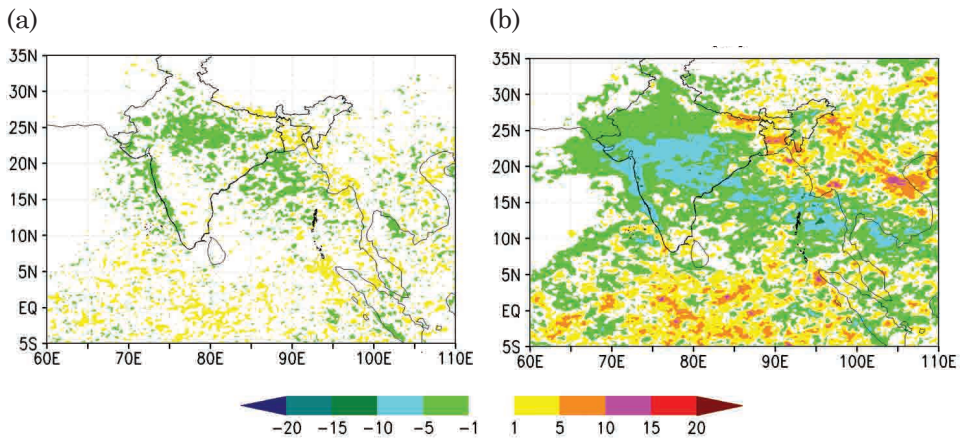


Figure 3. (a) Convective and (b) stratiform anomaly derived from 2A23 data, composited for break monsoon phases during July and August for the period 2002–2010. The anomalies of echo fractions are shown as percentage value.

latitude from 18 to 25° N for the lead-lag analysis of active/break episodes. Similar to the TRMM 3B42 dataset, this composite for all events is also created from daily values of $Q1$ and $Q2$ leading up to and following the active/break episodes. The first lead (lag) day is created with compositing data of one day prior to (following) the each active/break episode of study period. Similarly second lead (lag) day is created with compositing data, two day prior to (following) each episode of active/break for entire study period.

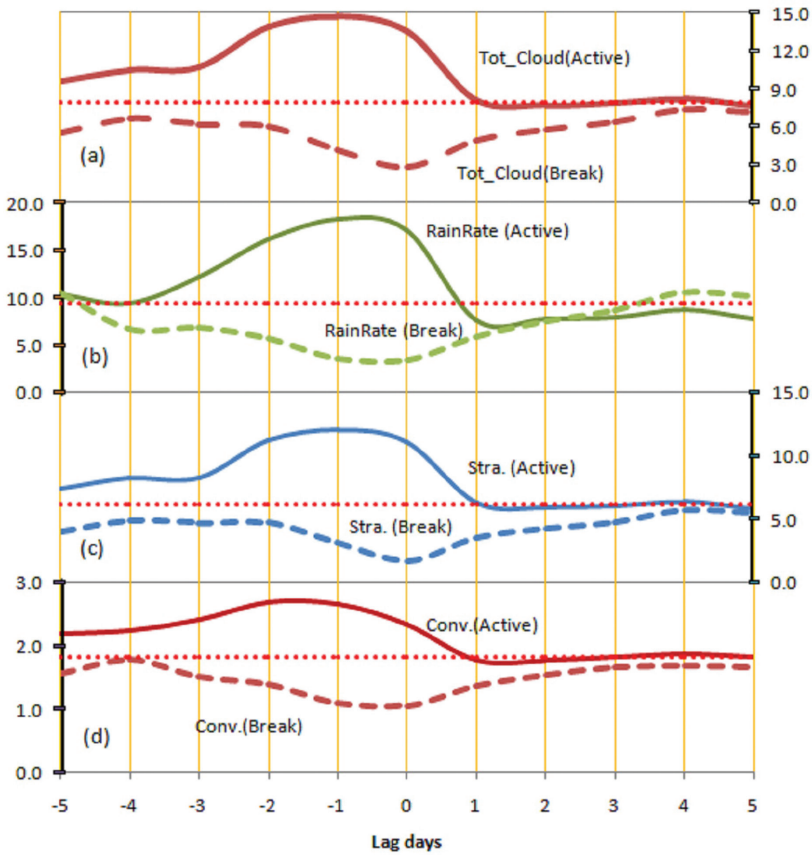


Figure 4. Lead-lag composite leading to, during, and following the active (solid line) and break (dashed line) phases, box averaged over the CMR for (a) total cloud percentage of total sample observed and (b) TRMM 3B42 rain rate in mm/day. (c) Stratiform and (d) convective percentage of total sample observed. Dotted horizontal lines are the corresponding climatological values.

3. Results and discussion

3.1. Variation of cloud pattern during active and break phase

The composite grid point anomaly maps, for the convective and stratiform cloud fraction for active and break phases are plotted in Figs. 2 and 3, respectively. The anomalies have been computed by subtracting the climatological value, (which is the composite value of the cloud fractions for that grid point computed from the entire daily data of July and August from 2002 to 2010) from the composite value of the cloud fractions for the all active/break days for the period. In the active period of ISM (Fig. 2), both stratiform and convective cloud anomaly is positive over central India and North Bay of Bengal (BoB) north of

10° N, indicating a general increase in the cloud cover over the region, compared to the foothills of Himalayas (FoH) and North-Eastern India (NEI), where they are negative. However, the relative increase in the stratiform fraction over its climatological value (as much as 20%) during this phase is greater than the corresponding increase in the convective cloudiness (up 5%). Earlier studies have noted that convection over the CTCZ region is generated in association with the movement of monsoon lows and depressions over the region during the active phase of monsoon. TRMM precipitation radar observations as well as various field experiments indicate that these clouds are organized into Mesoscale Convective Systems (MCS) with a relatively higher abundance of stratiform-type precipitation (mostly nimbostratus) clouds (Houze and Churchill, 1987; Houze, 1989). Simulation experiments using an atmospheric GCM show that the CTCZ responds dynamically to latent heating from mesoscale convective systems (MCSs) which suggest that a stratiform-type heating profile is very efficient in promoting upward development of continental-scale cyclonic circulation well above the midtroposphere over the MT region during the active phase of the ISM (Dey Choudhury and Krishnan, 2011). Over the west coast of India (WCI), the stratiform anomaly is negative (about -5%) off shore and positive (about +5%) over inland areas, and positive convective anomalies (about +5%) are observed during the active spell. On the WCI, the convective systems form windward of the terrain of Western-Ghat Mountain as an orographic response to the southwesterly monsoon flow, which develops inward of coast line. Earlier observational studies indicated that the ISM cloudiness over this region is mostly convective (Romatschke and Houze, 2011; Grossman and Durran, 1984). These studies noted that since the convection over this region is non-extreme in nature, they do not develop large stratiform outflows.

The anomaly pattern in the cloud fractions reverses during the break phase (Fig. 3). The stratiform and convective cloud fractions decrease (up to 20% and 5%, respectively) over central India and Bay of Bengal, while increasing over the foothills of the Himalayas and North East India. In this case too, the changeover is more significant in the stratiform cloud fractions (20%) as compared to the convective cloud fraction (5%), although the sign change in the anomaly is identical. Previous studies indicated the presence of clouds with smaller vertical extent (3–5 km) over the central Indian region during the break phase. These clouds are observed to occur in association with a heat low type circulation over this region (Rajeevan et al., 2013).

The above results indicate that the intensification and suppression of deep convective systems in the monsoon trough region, dictate the monsoon variability associated with active and break spells in the ISM. This is similar to the previous findings (Yasunari, 1980; Sikka and Gadgil, 1980). Since the variability of the cloud cover over the monsoon trough region appears to be a significant parameter in identifying the active/break phases of ISM, the variation of cloudiness over the monsoon trough region is analyzed in greater detail to identify signals preceding

the onset of active/break phase over the Indian subcontinent. A reference box is selected around the climatological position of the CTCZ during this season (18° N– 25° N and 65° E– 88° E). The coordinates and location of the box coincide with the reference box selected by Rajeevan et al. (2013) to define the active and break phases of ISM used for reference in this study. The box averaged percentage value of composite total, stratiform and convective cloudiness over this region (hereafter called Core Monsoon Region – CMR), before, during, and following the active and break phases is plotted in Fig. 4. This is compared with the daily rainrate values derived from 3B42 dataset for the same reference box.

As may be seen from the figure, the positive anomaly in the total cloud amount in the reference box (Fig. 4a), leads to the onset of the active phase of ISM by two to three triads and it is in phase with the accumulated rainfall for the same box (Fig. 4b). The corresponding anomaly in the cloud fractions also leads to the onset of active and break phases. However, for the active phase, while the increase in the stratiform fraction is in phase with the total cloud amount (Fig. 4c), and peaks about one triad before the actual onset, the convective fraction peaks about two triads prior to the onset of the active phase (Fig. 4d). The decay of the cloudiness and average rainrate at the cessation of the active phase, is in phase for all four components, i.e. the rainfall amount, total cloudiness, convective and stratiform fractions, are close to climatological values (or less, as in the case of the rainrate), in the first triad after cessation. This indicates the gradual buildup of the atmospheric conditions leading to the active phase and the sudden cession of such conditions, leading to the cession of the active phase. The peaking of the convective fraction of cloudiness, leading the stratiform fraction by one triad prior to the onset of the active phase indicates that initially the increase in the convective cloudiness over this region heralds the future onset of the active phase. As the system organization increases, the stratiform fraction increases, as does the general spread and amount of rainfall (in phase with the increase in the stratiform cloudiness). Romatschke and Houze (2011) also observed similar characteristics over the Indian monsoon region from TRMM observations, and inferred that the convective (stratiform) fraction decreases (increases) with the increasing system size. Recent studies (e.g., Lin et al., 2004; Abhik et al., 2012) using TRMM observational and NWP model reanalysis data have also documented the lead-lag relationship of convective and stratiform rainfall buildup at the onset of the ISM active phase. This is indicative of the presence of dynamical and thermodynamical forcing required for formation of large scale stratiform cloudiness much prior to the actual occurrence of cloudiness. However, the decrease in the convective and stratiform cloud fractions at the end of the active phase is very abrupt and rainfall decreases in the CMR region accordingly, indicating thus an abrupt cessation of dynamic conditions at the end of the active phase. Earlier study of Rao et al. (2004) has also documented that large scale drying occurs from middle to upper troposphere over the continental tropical convergence zone (CTCZ) three days before the cessation of

Table 2. Correlation coefficient between normalized pixels count values of convective, stratiform cloud amount, total cloud amount and rainfall for the CMR region.

Phase / Type	Convective vs. Stratiform	Convective vs. Rainfall	Stratiform vs. Rainfall	Total cloud vs. Rainfall
Active	0.928	0.900	0.981	0.978
Break	0.869	0.819	0.755	0.781

active spell. Hence, the process of cessation of active phase of ISM is initiated within the active phase itself.

The gradual buildup of atmospheric conditions, which is seen in the cloud and rain-rate parameters prior to the onset of the active phase, is also observed prior to the onset of the break phase. The negative anomaly in the cloud amount, rainrate, as well as individual stratiform and convective cloud fractions starts about 4 triads prior to the onset of the break phase. All the parameters are in phase with each other and attain maximum negative anomaly values at the onset of the break phase. The gradual shift towards the break phase, as indicated by the gradually increasing negative cloud anomalies, again indicates the presence of dynamical and thermodynamical forcing much in advance of the actual occurrence of the break phase. Also, unlike the active phase, the parameters do not show any sharp increase in values, and they only gradually reach the corresponding climatological mean values (after about four triads for the cloud parameters and four days for the rainrate) following the break spell.

Although, as Fig. 4 demonstrates, the cloud cover, the average rainrate, and the stratiform fraction of cloudiness for the CMR region are highly correlated with each other, leading to, at the onset of, and following the active and break phases, the correlation is stronger for active phase of ISM as compared to the break phase (Tab. 2). These findings are consistent with the results of previous studies showing that the stratiform rain coincides with higher total precipitation values (Romatschke and Houze, 2011; Dey Choudhury and Krishnan, 2011). One explanation for the poorer correlation during the break phase may be due to the fact that the cloudiness over the CMR region during the break phase results from short-lived thunderstorms. Their effect may not be captured very well by the twice-daily passes of the TRMM polar orbiting satellite.

It may also be observed in Fig. 4, that the composite frequency of occurrence of convective and stratiform precipitating clouds as well as the total rainfall over the CMR region peaks slightly before that actual onset of the active phase. However, comparing lag -2 image against corresponding lag 0 image of composite active phase (Fig. 7b of Rajeevan et al., 2010), visual inspection indicates that the magnitude of positive rainfall anomaly belt over central India slightly decreases with the onset of the active phase. This is not true for the break phase (Fig. 7a of

Rajeevan et al., 2010). Though they did not discuss this discrepancy in their paper, we believe that this arises due to the compositing of multiple events of different intensities of daily rainfall in obtaining the average pattern. However, this does not materially affect the main conclusions discussed in this section.

3.2. Variation of heat source (Q_1) and moisture sink (Q_2) in relation to the intraseasonal variability of the ISM

The strong correlation of the cloud fractions with the rainfall amount over the monsoon trough region indicates the strong role of the atmospheric heating profile in the variation of ISM rainfall. This indicates that the thermodynamic structure of the atmosphere gradually evolves with the approach of the active/break phase. Nitta (1983) showed that the long period fluctuations of the heat source over the eastern Tibetan Plateau are closely related to the intra-seasonal variation of the summer monsoon activity of 1979. Luo and Yanai (1984) identified that the principal components of heat sources over the Assam-Bengal region are primarily due to convection. Bhide et al. (1997) used the FGGE level III b data of the European Centre for Medium Range Weather Forecasts to show that the apparent heat source and the apparent moisture sink over the CTCZ area vary coherently with the rainfall over central India. They further suggested that the diabatic heating was largely contributed by the latent heat of cumulus convection.

The NCEP reanalysis model output is used to examine the variation of the atmosphere over the CMR region in terms of the apparent heat source and sink. As already stated in the introduction, the relative fractions of convective and stratiform cloudiness determine the level of maximum heating in the atmosphere. Before the re-analysis output is used for understanding the atmosphere, it is necessary to assess whether the vertical profile of apparent heat source - Q_1 and moisture sink - Q_2 computed from the re-analysis output matches the relative fractions of cloud amount as seen in the previous section. The box averaged vertical profile of the anomaly of Q_1 and Q_2 for the CMR region, averaged for all active and break periods is displayed in Fig. 5. Here too, the composite anomalies of Q_1 and Q_2 were computed with respect to the box averaged value of the grid point average value of the parameter computed using daily values for July and August from 2002 to 2010. As may be seen from the figure, positive anomaly values in the value of Q_1 (of the order of +3 K/day) are observed at 250 hPa during the active phase and negative anomaly values of the order of 3 K/day are seen at the same level during the break phase. The anomalously high Q_1 in the upper atmosphere during the active phase is typically associated with stratiform cloudiness. Their dominance during the active phase and decreased presence during the break phase (as seen in the previous section) matches the observed anomaly values of Q_1 . The point of inflection of Q_1 is at about 500 hPa, which is the freezing level during this season. The vertical profile of Q_2 has a double peaked curve during the active phase, with a larger maximum value of 2.5 K/day at the surface and a smaller peak of less negative values at 500 hPa. The vertical

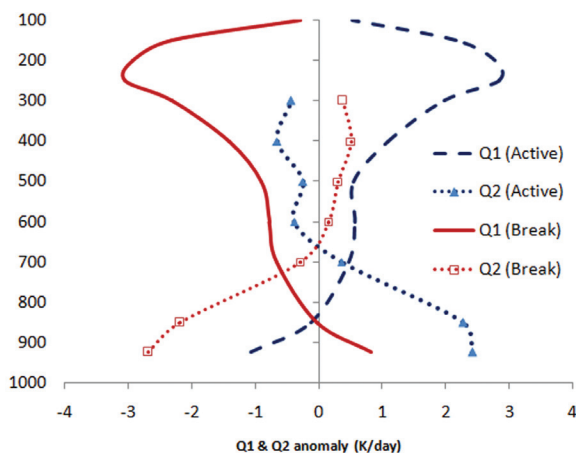


Figure 5. Average anomaly vertical profiles of $Q1$ and $Q2$ over CMR composited for active and break monsoon phases during July and August for the period 2002–2010. Here $Q1$ and $Q2$ values are in K/day and vertical pressure levels are in hPa.

profile of the moisture sink $Q2$ during the break phase is marked by strong negative anomalies (maximum at the surface ~ -2.8 K/day). The convective clouds give the lower drying peak in $Q2$ at the surface during the active phase. Their decreased fraction during the break phase, seen in the previous section, leads to the moistening of the lower atmosphere. Since profiles of $Q1$ and $Q2$ calculated using the NCEP re-analysis dataset match very well with the observed cloud pattern over the CMR region during the active and break phases, the evolution of the heating profile leading to, during, and following the active and break phases is studied in greater detail through the analysis of $Q1$ and $Q2$ along a vertical cross section through the monsoon core region between longitudes from 65 to 105° E averaged over 18 to 25° N. The profile of $Q1$ and $Q2$ during the active phase, as well as for five days leading to and following the same is displayed in Fig. 6 and Fig. 7, respectively. The most significant feature in the vertical section of $Q1$ profile is the negative heating anomaly in the lower atmosphere over the longitude belt of 85 – 95° E over the Bay of Bengal and adjoining land regions leading up to the active phase. The cooling starts on day 5, preceding the actual occurrence of the active phase, and gradually increases to a maximum on day 3 (~ -4 K/day below 700 hPa). It is superposed by a region of positive heating anomaly in the upper levels, which gradually builds up at longitudes west of 80° E ($+4$ K/day centred at 200 hPa). The negative anomaly region then shifts slightly westward and decreases in intensity at the onset of the active phase. There is corresponding drying of the lower troposphere as indicated by the positive values of the moisture sink $Q2$ over the same region ($+4$ K/day east of 85° E in Fig. 7). This region too, gradually shifts westward to over Orissa and adjoining regions, in phase with the westward shift of the cold anomaly of $Q1$. The collocated re-

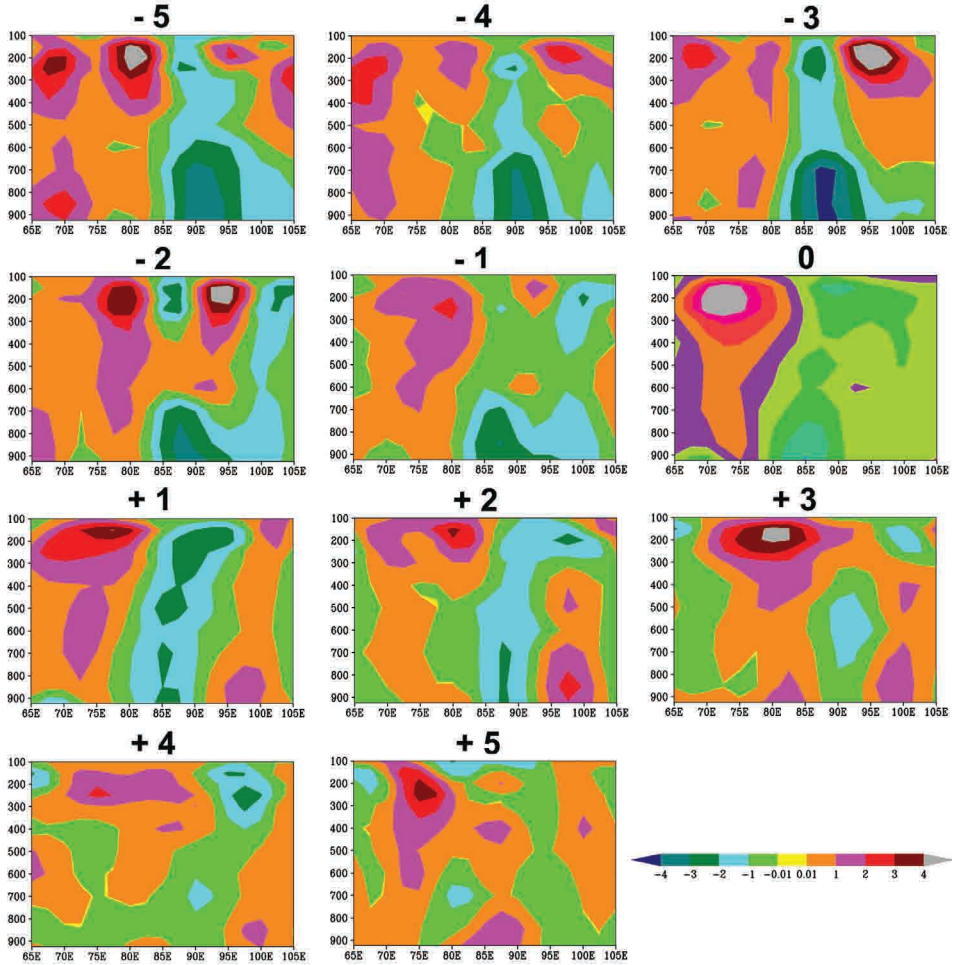


Figure 6. Lead and lag composite vertical cross-section profile of heat source (Q_1) anomaly for active phase averaged over latitude 18–25° N displayed between longitudes from 65 to 105° E. The anomaly values are in K/day and vertical pressure levels are in hPa.

gions of cooling anomaly in the value of Q_1 and drying in the low levels over the Bay of Bengal point to the formation of convective clouds over the region preceding the active phase. The model analysis points to their gradual buildup, leading up to two days preceding the onset of the active phase and decay thereafter. Also, of interest is the corresponding buildup of the upper tropospheric warming over longitudes west of 80° E, leading up to the active phase, which indicates a gradual increase in stratiform cloudiness over the western edge of the monsoon trough region which reaches a maximum during the active phase. This indicates that the engine for cloud growth during the monsoon season lies primarily in the

latent heat source from Bay of Bengal and adjoining east India. It also validates the inferences of the previous section of the role of the convective cloudiness in the initiation of the active phase. The onset of the active phase is primarily marked with the maximum growth of the stratiform region over the monsoon trough region. Following the cessation of the active phase, the cold anomaly region in the lower troposphere, east of 80° E moves westward, and is replaced by low level warming over East India (~ +1 to +2 K/day). Within the next 2 to 3 days the positive heating anomaly becomes negligible over the entire CMR. Simultaneously, the low level drying during active phase (as seen from the positive anomaly region in the Q_2 profile) shifts westward and negative anomalies in the value

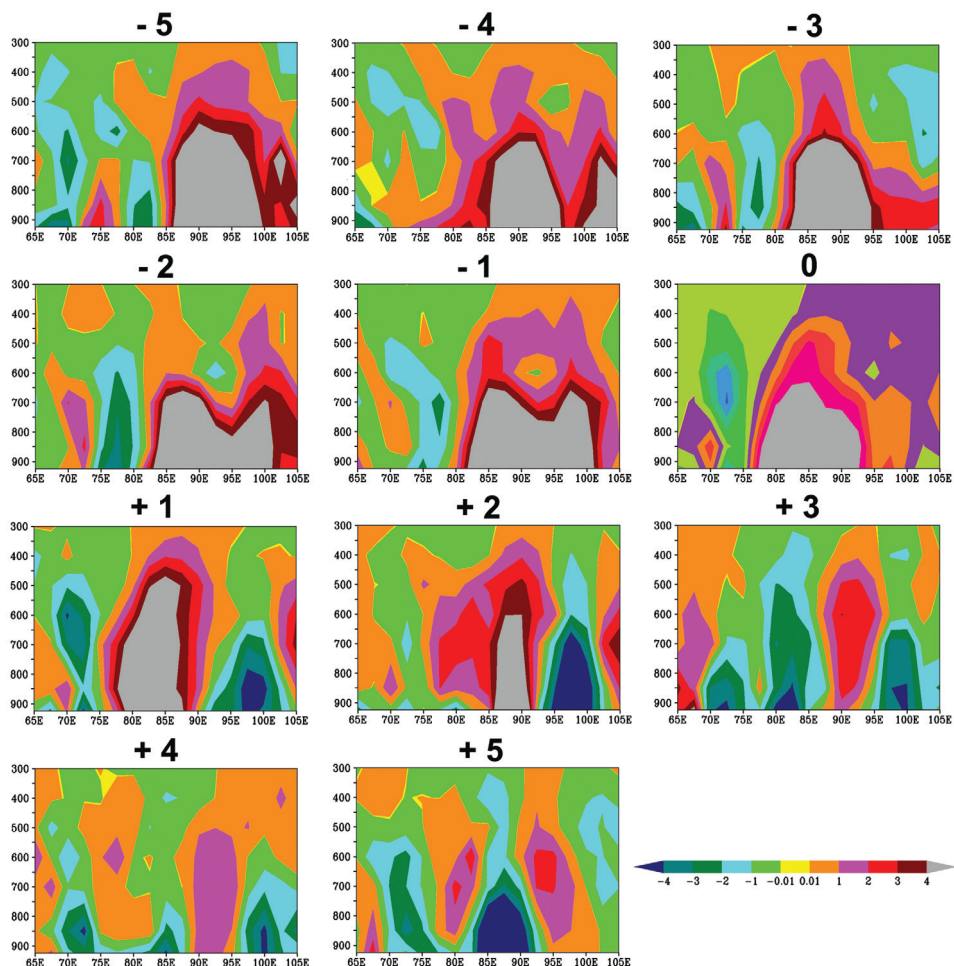


Figure 7. Same as Fig. 6, but for moisture sink (Q_2) anomaly of active phase.

of Q_2 , signifying moistening of the atmosphere become prominent. This indicates decreased convection over the CMR region at the end of the active phase.

Additionally, during the active phase, east of 75° E, a thin plume of negative Q_2 is seen at all levels with maximum values at 700 hPa (~ -4 K/day) indicating moistening of the atmosphere. The spatial pattern indicates that the moistening of the atmosphere is mostly over the cloud free zone of Rajasthan which is relatively free of convection during the active period. Another maximum in the positive anomaly of Q_2 is observed between 70 to 75° E, with maximum values at 850 hPa, which coincides with cooling in the lower troposphere (negative anom-

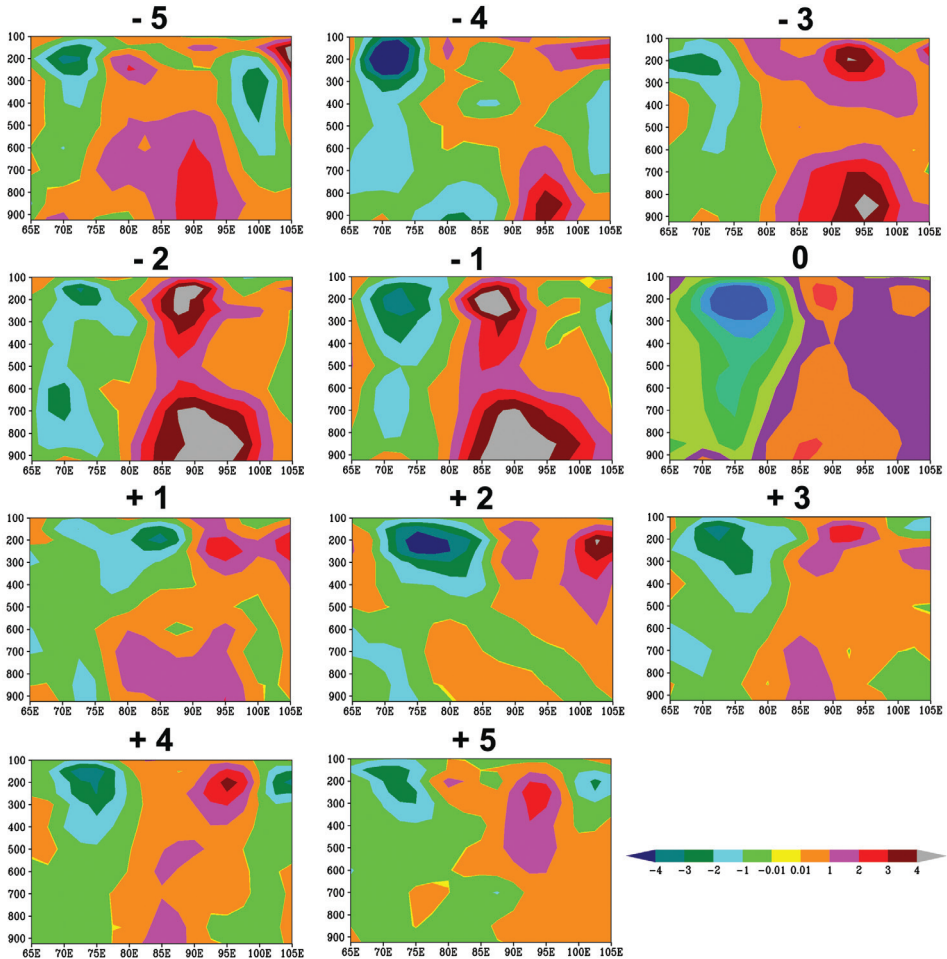


Figure 8. Lead and lag composite vertical cross-section profiles of heat source (Q_1) anomaly for break phase averaged over latitude 18 – 25° N displayed between longitudes from 65° to 105° E. The anomaly values are in K/day and vertical pressure levels are in hPa.

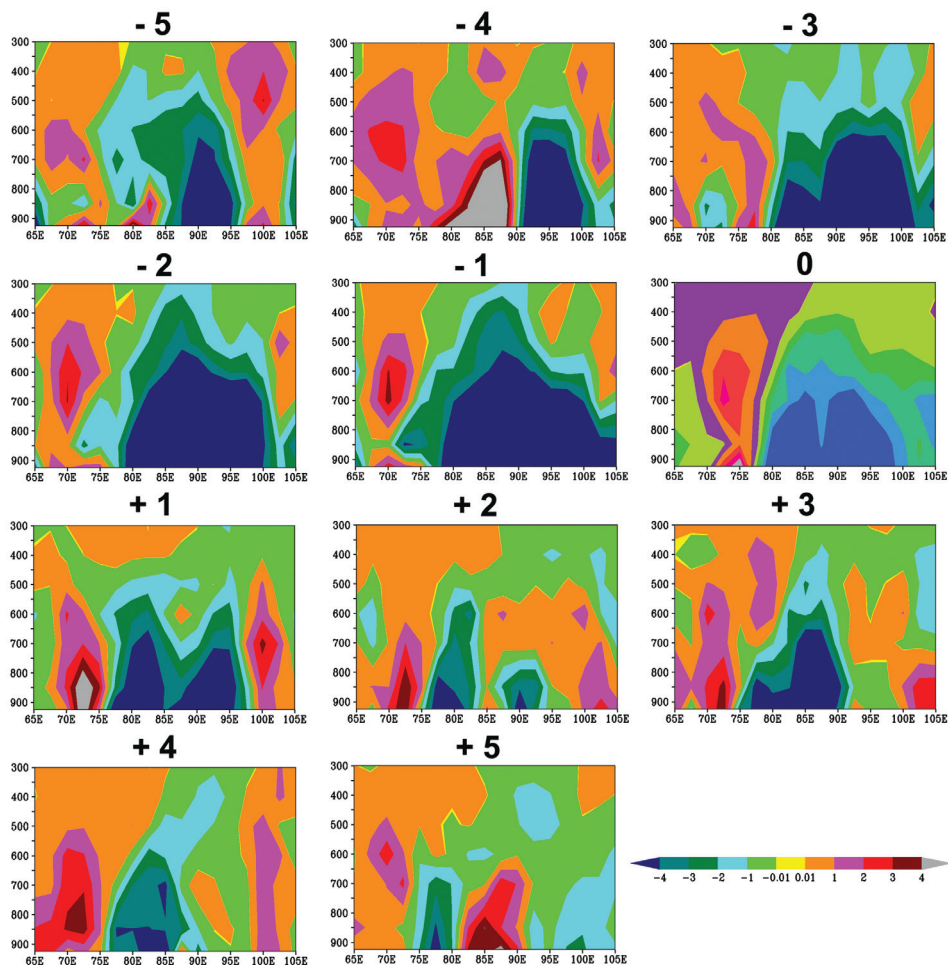


Figure 9. Same as Fig. 8, but for moisture sink (Q_2) anomaly of break phase.

ality of $Q_1 \sim 2\text{--}3$ K/day below 850 hPa). This region corresponds to the west coast of India. However, it may be noted, that unlike the cloudiness over the Bay of Bengal, the anomalies of Q_1 and Q_2 over this region are less intense and the maximum values are in-phase with the onset of the active phase. Studies using the data of INSAT 1B satellite indicate that the cloud systems over WCI region are characterized by weather systems which have their greatest intensity between 700 and 500 hPa (Francis and Gadgil, 2006).

The composite vertical profile of Q_1 and Q_2 , averaged over latitude $18\text{--}25^\circ$ N for the break phase, as well as for five days leading up to and following the same is displayed in Fig. 8 and Fig. 9, respectively. As with the active phase, signals

for the onset of the break phase begin to appear in the $Q1$ and $Q2$ profiles over the Bay of Bengal and east India, much in advance of the actual onset of the break phase. The days leading up to the break period are dominated by a gradually increasing positive heating anomaly in the value of $Q1$ at the lower levels, east of 80° E, which peaks on the day preceding the start of the break phase ($\sim +4$ K/day at the surface) and cools thereafter. The upper level cools, and a zone of strong cold anomalies develop, west of 80° E. The cooling is maximal during the break phase (-4 K/day at 200 hPa). The warm anomaly zone at the surface gradually decreases in intensity with the onset of the break phase, before decaying away altogether on the days following the break phase. The cold anomaly zone of $Q1$, which is maximum at the break phase, also decays at the end of the break phase. The corresponding profile of $Q2$ indicates a gradual buildup of moisture in the lower atmosphere to the east of 80° E (~ -3 K/day negative anomalies at the surface). The moist anomalies in the lower half of the troposphere and dry anomaly aloft are clearly related to shallow convection (Zhang and Mu, 2005). The negative anomaly zone in the value of $Q2$ at the surface decays and moves westward, following the cessation of the break phase of ISM. This is replaced by a zone of positive $Q2$ anomalies (indicating drying in the lower troposphere) between 80 and 90° E, which attains maximum value, about 5 days following the ISM break phase ($\sim +4$ K/day). A major characteristic of the break phase is the significant drying of the atmosphere to the west of 77° E. This zone persists throughout the approach, onset and withdrawal of the break phase, and coincides with a corresponding cooling of the atmospheric profile.

Previous studies have noted that leading to and during the active phase, the CTCZ is stronger, featuring cyclonic vorticity and enhanced convection, with low level vorticity maximum at the head Bay of Bengal (BoB) and extending along the CTCZ (e.g., Goswami and Ajaya Mohan, 2001). Experiments during the BOBMEX (Bay of Bengal Monsoon Experiment) also show that there are significant changes in the vertical temperature and relative humidity structure of the atmosphere between the active and weak convective conditions (Bhat et al., 2001). The head Bay of Bengal becomes the preferred zone of genesis of monsoon low pressure systems during the active phase of monsoon season and quiescent conditions prevail during the break phase. As the above analysis shows, the formation of organized cloud systems over this region, promotes the stratiform cloud growth thereby leading to the onset of the active phase of ISM. The westward propagation of the heat source and sink, which is observed in this study, closely matches the previous observations of westward propagation of heat sources and moisture sinks across the CTCZ with a periodicity closely linked to the intraseasonal variability of the ISM (Bhide et al., 1997). The development of a second zone over the North Arabian Sea, adjacent to Gujarat Coast of India, where cloudiness develops in-phase with the active spell over the monsoon zone, also matches previous observations (Gadgil and Joseph, 2003).

4. Conclusions

The clouds over the Indian subcontinent exhibit very distinctive pattern in respect to the type and spatial distribution in the course of ISM intra-seasonal variability. Analysis of observational TRMM PR data shows that the most significant difference in cloud cover between the active and break phase of ISM occurs over the monsoon trough region of the Indian subcontinent. Further, analysis shows that this significant changeover in the cloudiness, which is closely related to the rainfall rate, also extends to the amount of stratiform and convective cloudiness over the region. However, the increase/decrease in the cloud fractions, are not uniform for both types of clouds. The changeover between active or break phase conditions from the climatological distribution is more significant for the stratiform cloud fraction (~20%), which in turn is closely related to the relative increase and decrease of rainfall amount associated with the intra-seasonal variability of ISM. The change is less significant for convective cloudiness (~5%), and the maximums precede the actual onset of active phases. One may infer that deep MCS type convection producing large amount of stratiform clouds are prominent during the active phase of ISM, while shallow convection with less stratiform outflows, are the dominant cloud type during break spell. These properties of convection during active and break are also well reflected in heating profile of the atmosphere computed from the NCEP-NCAR reanalysis data.

While the composite profile corroborates the findings with respect to the cloud type dominance, the vertical section through the monsoon trough investigated region displays a distinct east-west variation in the vertical profile of the apparent heat source and moisture sink, which is in relation to the intra-seasonal variability of ISM. The analysis of the NCEP re-analysis data shows that the deep convection initiated on the eastern parts of CMR, i.e. Bay of Bengal and adjoining land areas 2–3 days prior to the onset of the active phase, moves westward up to the central India during active period. However, convection over western CMR (WCI and Arabian Sea) gradually builds up and is stationary over the same region with the onset of active period. On the other hand, the break phase is initiated with the moistening of low level along with positive heating anomaly on the eastern part of CMR and gradually moves westward. Hence, the heating profile over the Bay of Bengal and adjoining east India appears to be the most important prognostic indicator of the intra-seasonal variability of ISM. The dynamical and thermodynamical environment over the region is primarily responsible for the future onset of the active and break phases of the ISM.

Another significant lead-lag feature of clouds in succeeding the active/break events is that both the convective and stratiform cloudiness decrease to the corresponding climatological values after one day of cessation of active phase, whereas, they gradually match with the climatological mean after four days succeeding the break spell. Hence, the process of transition from active to normal is initiated within the active period itself. On the other hand the transition from

break to normal monsoon condition occurs with the gradual buildup of dynamical and thermo-dynamical condition for normal monsoon flow. The findings of this study are expected to serve as important predictive signs of the onset and withdrawal of active/break phase of monsoon.

Acknowledgements – The authors are grateful to the Director General of Meteorology, India Meteorological Department, for constant encouragement during the course of this study. We are grateful to a large number of officers and other staff members at IMD, New Delhi. We are thankful to NASA Tropical Rainfall Measuring Mission's Goddard Earth Sciences Data and Information Services Center (GESDISC) for providing TRMM data for this project. We also acknowledge the NCEP Reanalysis data provided by the NOAA/OAR/ESRL PSD, Boulder, Colorado, USA, from their Web site at <http://www.esrl.noaa.gov/psd/>.

References

- Abhik, S., Halder, M., Mukhopadhyay, P., Jiang, X. and Goswami, B. N. (2013): A possible new mechanism for northward propagation of boreal summer intraseasonal oscillations based on TRMM and MERRA reanalysis, *Clim. Dynam.*, **40**, 1611–1624, DOI: [10.1007/s00382-012-1425-x](https://doi.org/10.1007/s00382-012-1425-x).
- Ananthakrishnan, R. (1977): Some aspects of the monsoon circulation and monsoon rainfall, *Pure Appl. Geophys.*, **115**, 1209–1249, DOI: [10.1007/BF00874407](https://doi.org/10.1007/BF00874407).
- Anders, A. M., Roe, G. H., Hallet, B., Montgomery D. R., Finnegan N. J. and Putkonen, J. (2006): Spatial patterns of precipitation and topography in the Himalaya, *Tectonics, Climate, and Landscape Evolution: Geological Society of America Special Paper*, **398**, 39–53, DOI: [10.1130/2006.2398\(03\)](https://doi.org/10.1130/2006.2398(03)).
- Annamalai, H., Slingo, J. M., Sperber, K. R. and Hodges, K. (1999): The mean evolution and variability of the Asian summer monsoon: Comparison of ECMWF and NCEP–NCAR reanalyses, *Mon. Wea. Rev.*, **127**, 1157–1186, DOI: [10.1175/1520-0493\(1999\)127<1157:TMEAVO>2.0.CO;2](https://doi.org/10.1175/1520-0493(1999)127<1157:TMEAVO>2.0.CO;2).
- Awaka, J., Iguchi, T., Kumagai, H. and Okamoto, K. (1997): Rain type classification algorithm for TRMM precipitation radar, *Geoscience and Remote Sensing, 1997: IGARSS '97, Remote Sensing – A Scientific Vision for Sustainable Development*, **4**, 1633–1635, DOI: [10.1109/IGARSS.1997.608993](https://doi.org/10.1109/IGARSS.1997.608993).
- Bell, T. L. and Kundu, P. K. (2000): Dependence of satellite sampling error on monthly averaged rain rates: Comparison of simple models and recent studies, *J. Climate*, **13**, 449–462, DOI: [10.1175/1520-0442\(2000\)013<0449:DOSSEO>2.0.CO;2](https://doi.org/10.1175/1520-0442(2000)013<0449:DOSSEO>2.0.CO;2).
- Bhat, G. S., Gadgil, S., Hareesh Kumar, P. V. H., Kalsi, S. R., Madhusoodanan, P., Murty, V. S. N., Rao, C. V. K. P., Rameshbabu, V., Rao, L. V. G., Rao, R. R., Ravichandran, M., Reddy, K. G., Sanjeeva Rao, P., Sengupta, D., Sikka, D. R., Swain, J. and Vinayachandran, P. N. (2001): BOBMEX: the Bay of Bengal monsoon experiment, *Bull. Amer. Meteor. Soc.*, **82**, 2217–2243, DOI: [0.1175/1520-0477\(2001\)082<2217:BTBOBM>2.3.CO;2](https://doi.org/10.1175/1520-0477(2001)082<2217:BTBOBM>2.3.CO;2).
- Bhide, U. V., Majumdar, V. R., Chanekar, S. P., Paul, D. K., Chen, T. C. and Rao, G. V. (1997): A diagnostic study on heat sources and moisture sinks in the monsoon trough area during active-break phases of the Indian summer monsoon, 1979, *Tellus*, **49A**, 455–473, DOI: [10.1034/j.1600-0870.1997.t01-2-00004.x](https://doi.org/10.1034/j.1600-0870.1997.t01-2-00004.x).
- Bowman, K. P., Collier, J. C., North, G. R., Wu, Q., Ha, E. and Hardin, J. (2005): Diurnal cycle of tropical precipitation in Tropical Rainfall Measuring Mission (TRMM) satellite and ocean buoy rain gauge data, *J. Geophys. Res.*, **110**, D21104, DOI: [10.1029/2005JD005763](https://doi.org/10.1029/2005JD005763).
- Chattopadhyay, R., Goswami, B. N., Sahai, A. K. and Fraedrich, K. (2009): Role of stratiform rainfall in modifying the northward propagation of monsoon intraseasonal oscillation, *J. Geophys. Res.*, **114**, D19114, DOI: [10.1029/2009JD011869](https://doi.org/10.1029/2009JD011869).
- Dey Choudhury, A. and Krishnan, R. (2011): Dynamical response of the South Asian monsoon trough to latent heating from stratiform and convective precipitation, *J. Atmos. Sci.*, **68**, 1347–1363, DOI: [10.1175/2011JAS3705.1](https://doi.org/10.1175/2011JAS3705.1).

- Francis, P. A. and Gadgil, S. (2006): Intense rainfall events over the west coast of India, *Meteorol. Atmos. Phys.*, **94**, 27–42, DOI: [10.1007/S00703-005-0167-2](https://doi.org/10.1007/S00703-005-0167-2).
- Gadgil, S. (2003): The Indian monsoon and its variability, *Annu. Rev. Earth Pl. Sc.*, **31**, 429–467, DOI: [10.1146/annurev.earth.31.100901.141251](https://doi.org/10.1146/annurev.earth.31.100901.141251).
- Gadgil, S. and Joseph, P. V. (2003): On breaks of the Indian monsoon, *J. Earth Syst. Sci.*, **112**, 529–558, DOI: [10.1007/BF02709778](https://doi.org/10.1007/BF02709778).
- Goswami, B. N. and Ajaya Mohan, R. S. (2001): Intraseasonal oscillations and interannual variability of the Indian summer monsoon, *J. Clim.*, **14**, 1180–1198, DOI: [10.1175/1520-0442\(2001\)014<1180:IOAIVO>2.0.CO;2](https://doi.org/10.1175/1520-0442(2001)014<1180:IOAIVO>2.0.CO;2).
- Grossman, R. L. and Durran, D. R. (1984): Interaction of low-level flow with the western Ghat Mountains and offshore convection in the summer monsoon, *Mon. Wea. Rev.*, **112**, 652–672, DOI: [10.1175/1520-0493\(1984\)112<0652:IOLEFW>2.0.CO;2](https://doi.org/10.1175/1520-0493(1984)112<0652:IOLEFW>2.0.CO;2).
- Houze Jr., R. A., Cheng, C. P., Leary, C. A. and Gamache, J. F. (1980): Diagnosis of cloud mass and heat fluxes from radar and synoptic data, *J. Atmos. Sci.*, **37**, 754–773, DOI: [10.1175/1520-0469\(1980\)037<0754:DOCMHA>2.0.CO;2](https://doi.org/10.1175/1520-0469(1980)037<0754:DOCMHA>2.0.CO;2).
- Houze Jr., R. A. (1982): Cloud clusters and large-scale vertical motions in the Tropics, *J. Meteor. Soc. Jpn.*, **60**, 396–410.
- Houze Jr., R. A. and Churchill, D. D. (1987): Mesoscale organization and cloud microphysics in a Bay of Bengal depression, *J. Atmos. Sci.*, **44**, 1845–1868, DOI: [10.1175/1520-0469\(1987\)044<1845:MOACMI>2.0.CO;2](https://doi.org/10.1175/1520-0469(1987)044<1845:MOACMI>2.0.CO;2).
- Houze Jr., R. A. (1989): Observed structure of mesoscale convective systems and implications for large-scale heating, *Q. J. R. Meteorol. Soc.*, **115**, 425–461, DOI: [10.1002/qj.49711548702](https://doi.org/10.1002/qj.49711548702).
- Huffman, G. J., Adler, R. F., Bolvin, D. T., Gu, G., Nelkin, E. J., Bowman, K. P., Hong, Y., Stocker, E. F. and Wolff, D. B. (2007): The TRMM multisatellite precipitation analysis (TMPA): Quasi-global, multiyear, combined-sensor precipitation estimates at fine scales, *J. Hydrometeorol.*, **8**, 38–55, DOI: [10.1175/JHM560.1](https://doi.org/10.1175/JHM560.1).
- Johnson, R. H., Rickenbach, T. M., Rutledge, S. A., Ciesielski, P. E. and Schubert, W. H. (1999): Trimodal characteristics of tropical convection, *J. Climate*, **12**, 2397–2418, DOI: [10.1175/1520-0442\(1999\)012<2397:TCOTC>2.0.CO;2](https://doi.org/10.1175/1520-0442(1999)012<2397:TCOTC>2.0.CO;2).
- Kalnay, E. and Coauthors (1996): The NCEP/NCAR 40-Year Reanalysis Project, *Bull. Amer. Meteor. Soc.*, **77**, 437–471, DOI: [10.1175/1520-0477\(1996\)077<0437:TNYRP>2.0.CO;2](https://doi.org/10.1175/1520-0477(1996)077<0437:TNYRP>2.0.CO;2).
- Krishnamurthy, V. and Shukla, J. (2000): Intraseasonal and interannual variability of rainfall over India, *J. Climate*, **13**, 4366–4377, DOI: [10.1175/1520-0442\(2000\)013<0001:IAIVOR>2.0.CO;2](https://doi.org/10.1175/1520-0442(2000)013<0001:IAIVOR>2.0.CO;2).
- Krishnamurti, T. N. and Bhalme, H. N. (1976): Oscillations of a monsoon system. Part I: Observational aspects, *J. Atmos. Sci.*, **33**, 1937–1954, DOI: [10.1175/1520-0469\(1976\)033<1937:OOAmsP>2.0.CO;2](https://doi.org/10.1175/1520-0469(1976)033<1937:OOAmsP>2.0.CO;2).
- Krishnan, R., Zhang, C. and Sugi, M. (2000): Dynamics of breaks in the Indian summer monsoon, *J. Atmos. Sci.*, **57**, 1354–1372, DOI: [10.1175/1520-0469\(2000\)057<1354:DOBITI>2.0.CO;2](https://doi.org/10.1175/1520-0469(2000)057<1354:DOBITI>2.0.CO;2).
- Kummerow, C., Barnes, W., Kozu, T., Shiue, J. and Simpson, J. (1998): The Tropical Rainfall Measuring Mission (TRMM) sensor package, *J. Atmos. Oceanic Technol.*, **15**, 809–817, DOI: [10.1175/1520-0426\(1998\)015<0809:TTRMMT>2.0.CO;2](https://doi.org/10.1175/1520-0426(1998)015<0809:TTRMMT>2.0.CO;2).
- Lin, J., Mapes, B., Zhang, M. and Newman, M. (2004): Stratiform precipitation, vertical heating profiles, and the Madden–Julian oscillation, *J. Atmos. Sci.*, **61**, 296–309, DOI: [10.1175/1520-0469\(2004\)061<0296:SPVHPA>2.0.CO;2](https://doi.org/10.1175/1520-0469(2004)061<0296:SPVHPA>2.0.CO;2).
- Luo, H. and Yanai, M. (1984): The large-scale circulation and heat sources over the Tibetan Plateau and surrounding areas during the early summer of 1979. Part II: Heat and moisture budgets, *Mon. Wea. Rev.*, **112**, 966–989, DOI: [10.1175/1520-0493\(1984\)112<0966:TLSCAH>2.0.CO;2](https://doi.org/10.1175/1520-0493(1984)112<0966:TLSCAH>2.0.CO;2).
- Manoj, M. G., Devara, P. C. S., Safai, P. D. and Goswami, B. N. (2011): Absorbing aerosols facilitate transition of Indian monsoon breaks to active spells, *Clim. Dynam.*, **37**, 2181–2198, DOI: [10.1007/s00382-010-0971-3](https://doi.org/10.1007/s00382-010-0971-3).

- Nair, S., Srinivasan, G. and Nemani, R. (2009): Evaluation of multi-satellite TRMM derived rainfall estimates over a Western State of India, *J. Meteorol. Soc. Jpn.*, **87**, 927–939, DOI: [10.2151/jmsj.87.927](https://doi.org/10.2151/jmsj.87.927).
- Negri, A. J., Bell, T. L. and Xu, L. (2002): Sampling of the diurnal cycle using TRMM, *J. Atmos. Oceanic Technol.*, **19**, 1333–1344, DOI: [10.1175/1520-0426\(2002\)019<1333:SOTDCO>2.0.CO;2](https://doi.org/10.1175/1520-0426(2002)019<1333:SOTDCO>2.0.CO;2).
- Nesbitt, S. W. and Anders, A. M. (2009): Very high resolution precipitation climatologies from the Tropical Rainfall Measuring Mission precipitation radar, *Geophys. Res. Lett.*, **36**, L15815, DOI: [10.1029/2009GL038026](https://doi.org/10.1029/2009GL038026).
- Nitta, T. (1983): Observational study of heat sources over the eastern Tibetan Plateau during the summer monsoon, *J. Meteorol. Soc. Jpn.*, **61**, 590–605.
- Pokhrel, S. and Sikka, D. R. (2013): Variability of the TRMM-PR total and convective and stratiform rain fractions over the Indian region during the summer monsoon, *Clim. Dynam.*, **41**, 21–44, DOI: [10.1007/S00382-012-1502-1](https://doi.org/10.1007/S00382-012-1502-1).
- Raghavan, K. (1967): Influence of tropical storms on monsoon rainfall in India, *Weather*, **22**, 250–256, DOI: [10.1002/j.1477-8696.1967.tb02929.x](https://doi.org/10.1002/j.1477-8696.1967.tb02929.x).
- Rahman, S. H., Sengupta, D. and Ravichandran, M. (2009): Variability of Indian summer monsoon rainfall in daily data from gauge and satellite, *J. Geophys. Res.*, **114**, D17113, DOI: [10.1029/2008JD011694](https://doi.org/10.1029/2008JD011694).
- Rajeevan, M., Gadgil, S. and Bhate, J. (2010): Active and break spells of the Indian summer monsoon, *J. Earth Syst. Sci.*, **119**, 229–247, DOI: [10.1007/S12040-010-0019-4](https://doi.org/10.1007/S12040-010-0019-4).
- Rajeevan, M., Rohini, P., Niranjana Kumar, K., Srinivasan, J. and Unnikrishnan, C. K. (2013): A study of vertical cloud structure of the Indian summer monsoon using CloudSat data, *Clim. Dynam.*, **40**, 637–650, DOI: [10.1007/s00382-012-1374-4](https://doi.org/10.1007/s00382-012-1374-4).
- Ramamurthy, K. (1969): Some aspects of “break” in the Indian southwest monsoon during July and August, *Forecasting Manual, Indian Meteorological Department Publication, FMU, Rep. 4*, 18.3. [Available from Indian Meteorological Department, MausamBhavan, Lodi Road, New Delhi 110 003, India.]
- Rao, K. G., Desbois, M., Roca, R. and Nakamura, K. (2004): Upper tropospheric drying and the “transition to break” in the Indian summer monsoon during 1999, *Geophys. Res. Lett.*, **31**, L03206, DOI: [10.1029/2003GL018269](https://doi.org/10.1029/2003GL018269).
- Ravi Kiran, V., Rajeevan, M., VijayaBhaskara Rao, S. and Prabhakara Rao, N. (2009): Analysis of variations of cloud and aerosol properties associated with active and break spells of Indian summer monsoon using MODIS data, *Geophys. Res. Lett.*, **36**, L09706, DOI: [10.1029/2008GL037135](https://doi.org/10.1029/2008GL037135).
- Romatschke, U., Medina, S. and Houze, R. A. (2010): Regional, seasonal, and diurnal variations of extreme convection in the South Asian region, *J. Climate*, **23**, 419–439, DOI: [10.1175/2009JCLI3140.1](https://doi.org/10.1175/2009JCLI3140.1).
- Romatschke, U. and Houze, R. A. (2011): Characteristics of precipitating convective systems in the South Asian monsoon, *J. Hydrometeorol.*, **12**, 3–26, DOI: [10.1175/2010JHM1289.1](https://doi.org/10.1175/2010JHM1289.1).
- Schumacher, C. and Houze Jr., R. A. (2003): Stratiform rain in the tropics as seen by the TRMM precipitation radar, *J. Climate*, **16**, 1739–1756, DOI: [10.1175/1520-0442\(2003\)016<1739:SRITTA>2.0.CO;2](https://doi.org/10.1175/1520-0442(2003)016<1739:SRITTA>2.0.CO;2).
- Sikka, D. R. and Gadgil, S. (1980): On the maximum cloud zone and the ITCZ over Indian longitudes during the southwest monsoon, *Mon. Wea. Rev.*, **108**, 1840–1853, DOI: [10.1175/1520-0493\(1980\)108<1840:OTMCZA>2.0.CO;2](https://doi.org/10.1175/1520-0493(1980)108<1840:OTMCZA>2.0.CO;2).
- Steiner, M., Houze Jr., R. A. and Yuter, S. E. (1995): Climatological characterization of three-dimensional storm structure from operational radar and rain gauge data, *J. Appl. Meteor.*, **34**, 1978–2007, DOI: [10.1175/1520-0450\(1995\)034<1978:CCOTDS>2.0.CO;2](https://doi.org/10.1175/1520-0450(1995)034<1978:CCOTDS>2.0.CO;2).
- Webster, P. J., Magana, V. O., Palmer, T. N., Shukla, J., Tomas, R. A., Yanai, M. and Yasunari, T. (1998): Monsoons: Processes, predictability, and the prospects for prediction, *J. Geophys. Res.-Oceans*, **103**, 14451–14510, DOI: [10.1029/97JC02719](https://doi.org/10.1029/97JC02719).
- Yanai, M., Esbensen, S. and Chu, J. H. (1973): Determination of bulk properties of tropical cloud clusters from large-scale heat and moisture budgets, *J. Atmos. Sci.*, **30**, 611–627, DOI: [10.1175/1520-0469\(1973\)030<0611:DOBPOT>2.0.CO;2](https://doi.org/10.1175/1520-0469(1973)030<0611:DOBPOT>2.0.CO;2).

- Yasunari, T. (1980): A quasi stationary appearance of the 30–40 day period in the cloudiness fluctuation during the summer monsoon over India, *J. Meteorol. Soc. Jpn.*, **58**, 225–229.
- Zhang, G. J. and Mu, M. (2005): Simulation of the Madden–Julian oscillation in the NCAR CCM3 using a revised Zhang–McFarlane convection parameterization scheme, *J. Climate*, **18**, 4046–4064, DOI: [10.1175/JCLI3508.1](https://doi.org/10.1175/JCLI3508.1).

SAŽETAK

Unutarsezonska varijabilnost naoblake nad indijskim potkontinentom tijekom monsunse sezone na temelju mjerenja oborine radarom TRMM

Subhendu Brata Saha, Soma Sen Roy, S. K. Roy Bhowmik i P. K. Kundu

U radu je ispitana unutarsezonska varijabilnost indijskog ljetnog monsuna, koja se očituje izmjenom „aktivnih“ faza i faza „stanke“ u polju oborine, obzirom na varijabilnost konvektivne i stratiformne naoblake nad razmatranim područjem. U tu su svrhu analizirane monsunse sezone nad indijskim potkontinentom za razdoblje od 2002. do 2010. godine na temelju dugačkog niza podataka dobivenih pomoću satelita TRMM PR (podaci 2A23 i 3B42). Pokazano je da se najznačajnije prostorne promjene konvektivne i stratiformne naoblake povezane s aktivnom fazom i fazom stanke javljaju u području monsunse doline u polju tlaka zraka nad središnjom Indijom. Aktivnu fazu karakteriziraju pozitivne anomalije konvektivne (~5%) i stratiformne (~20%) naoblake. Međutim, maksimum konvektivne naoblake prethodi maksimumu stratiformne naoblake i javlja se 1–2 dana prije nastupa same aktivne faze, što ukazuje na to da do porasta stratiformne naoblake dolazi zbog postepenog organiziranja sustava konvektivne naoblake nad razmatranim područjem. Fazi stanke prethode dani s negativnim anomalijama konvektivne i stratiformne naoblake nad razmatranim područjem, a njihov je razvoj istovremen s razlikom od aktivne faze, kojoj prethode pozitivne anomalije konvektivne naoblake. Analiza polja atmosferskih izvora i ponora topline na temelju podataka NCEP–NCAR reanalize ukazala je na Bengalski zaljev i istočnu Indiju kao područja s glavnim uzročnicima porasta/smanjenja konvekcije u području monsunse doline u polju tlaka zraka. Aktivnoj fazi prethodi raspodjela izvora i ponora topline, koja podržava razvoj sustava velike skale, te sustavni porast konvektivne naoblake nad Bengalskim zaljevom, koji prethodi njenom samom početku, dok fazi stanke prethodi takva raspodjela izvora i ponora topline koja podržava razvoj izoliranih konvektivnih oblaka i potiskuje organizirano formiranje sustava oblaka nad područjem monsunse doline u polju tlaka zraka.

Ključne riječi: unutarsezonska varijabilnost, TRMM radar za mjerenje oborine, indijski ljetni monsun, aktivna faza, faza stanke, konvektivna naoblaka, stratiformna naoblaka, izvori topline, ponori topline

Corresponding author's address: Soma Sen Roy, India Meteorological Department, Lodi Road, New Delhi-3, India; e-mail: senroys@gmail.com